

Article

Biopolymeric Membranes with Active Principle of Olive Leaves (*Olea europaea* L.) for Potential Topical Application

Rafael Carvalho Alves ¹, Camila Ramão Contessa ² , Caroline Costa Moraes ²  and Gabriela Silveira da Rosa ^{1,*} 

¹ Science and Engineering of Materials Graduate Program, Laboratory of Chemical Engineering, Federal University of Pampa, P.O. Box 1650, Bagé 96413170, RS, Brazil; rafaelalvessete@hotmail.com

² Science and Engineering of Materials Graduate Program, Laboratory of Microbiology and Food Toxicology, Federal University of Pampa, P.O. Box 1650, Bagé 96413170, RS, Brazil

* Correspondence: gabrielarosa@unipampa.edu.br

Abstract: The biggest challenge for scientists is to create an ideal wound dressing that should be non-toxic, biocompatible, and biodegradable, providing optimal conditions for the most effective regeneration process. Biomaterials loaded with plant-derived compounds show better biocompatibility and biological properties, ensuring a faster tissue repair process. In order to develop membranes with good mechanical properties and anti-bacterial properties, the objective of this work describes the synthesis of a chitosan-based membrane added with olive leaf extract as an active principle with potential for topical application. The material developed was characterized in terms of morphology, physical, chemical, and mechanical properties, and the anti-bacterial capacity of the membranes. The results indicated that the developed membrane has good potential for use as a wound dressing, as it presented mechanical properties (30.17 ± 8.73 MPa) and fluid draining capacity (29.31 ± 1.65 g·m⁻²·h⁻¹) adequacy. In addition, the antimicrobial activity analysis revealed the active membrane potential against *E. coli* and *S. aureus* reaching 9.9 mm and 9.1 mm, respectively, in inhibition zones, the most common bacteria in skin wounds. Therefore, all the results indicate that the developed membrane presents viable characteristics for the use of wound dressing.

Keywords: anti-bacterial; bioactive; chitosan; olive leaves; wound healing



Citation: Alves, R.C.; Contessa, C.R.; Moraes, C.C.; Rosa, G.S.d.

Biopolymeric Membranes with Active Principle of Olive Leaves (*Olea europaea* L.) for Potential Topical Application. *Macromol* **2023**, *3*, 314–325. <https://doi.org/10.3390/macromol3020020>

Academic Editors: Paul Joseph, Svetlana Tretsiakova-McNally and Malavika Arun

Received: 31 March 2023

Revised: 17 May 2023

Accepted: 23 May 2023

Published: 1 June 2023



Copyright: © 2023 by the authors. Licensee MDPI, Basel, Switzerland. This article is an open access article distributed under the terms and conditions of the Creative Commons Attribution (CC BY) license (<https://creativecommons.org/licenses/by/4.0/>).

1. Introduction

The skin acts as a barrier to the external environment protecting all the internal organs of the body, and constitutes the largest tissue in the human body, representing 8% of the total body weight [1,2]. The wound is characterized when there is a break in the skin, where several restructuring processes begin. The restoration of metabolism occurs in stages: (i) Homeostasis, where there is a contraction of blood vessels and secretion of some compounds responsible for platelet activation and aggregation, and clot formation. (ii) Inflammation, where the release of amines and histamines responsible for the red coloration, heat, and swelling occurs; the attraction of neutrophils that phagocytose macrophages that secrete pro-inflammatory cytokines occurs. (iii) Proliferation, where it triggers epithelialization, regeneration of damaged capillary beds, and formation of new blood vessels. (iv) Tissue remodeling, where there is an increase in collagen, improving structural integrity and ending the healing process [3].

All chronic wounds are colonized by bacteria, microorganisms from the microbiota, and opportunists such as pathogenic bacteria, causing an acute inflammatory process referred to as infection [4]. *Staphylococcus aureus*, *Klebsiella pneumoniae*, *Pseudomonas aeruginosa*, and *Escherichia coli* have predominantly been isolated from infection and skin wounds. Unwanted contamination can lead to a prolongation of the inflammatory process, preventing wound healing, in addition to serious toxic effects when bacterial toxins reach the subcutaneous layer of the skin and pass into the bloodstream [5].

The use of antimicrobial dressings helps in the healing and prevention of skin infection and is essential in chronic wounds, which have a very long time in the inflammatory phase, such as in individuals with diabetes, for example [6,7]. When the wound is open or involved in a dry-type dressing process, healing is slower compared to a wet-type dressing process [8]. According to Moholkar et al. [9], an ideal dressing should present (i) a moist wound environment, (ii) permeability to gases for an exchange of oxygen, (iii) capacity to absorb exudates, (iv) act as a barrier to the penetration of microorganisms, and (v) reduce healing time.

Dressings based on biopolymer materials can provide faster healing due to their great ability to absorb tissue exudates, thus avoiding dehydration of the wound, allowing the permeation of oxygen and the release of active compounds, thus providing oxygenation of the wound, without external contamination, since they have the ability to form bioactive complexes with extracts for this purpose, due to their ionic character, thus maintaining favorable and necessary conditions for skin homeostasis and re-establishment of its integrity [8,10]. Chitosan is a natural polymer obtained from the deacetylation of chitin, extracted mainly from the shell of shrimp, is widely used in several areas, has good chemical properties, and stands out for its biocompatibility. Chitosan-based dressing membranes are good candidates for wound-healing dressings due to their biocompatibility, biodegradability, hemostatic and antimicrobial activity, and non-toxicity [11].

Olive leaves have been highlighted by the levels of biophenols, which have antioxidant [12], anti-bacterial [13], and anti-inflammatory [14] potentials. Olive leaf has a higher polyphenol content than extra virgin olive oil and the whole fruit [15], with oleuropein being the main phenolic extracted [16]. The leaves correspond to 10% of the total amount of olives that enter the oil industry [17] and correspond to the main by-product of the production process [18]. Their bioactive compounds have the potential for application in several areas, such as the food, biomedical, and nutraceutical industries [16,19]. The literature has already reported the use of olive leaf extract in films, and they discovered that these films could be used as antimicrobial food packaging [13,20]. However, there is a lack of research on the applicability of olive leaf extract in chitosan biopolymer membranes for wound dressing application.

Therefore, in order to add value to the by-products from the production of olives and olive oils combined with a global concern with environmental issues, the objective of this work is to bring a new perspective to the viability of the synthesis of a chitosan-based membrane (natural polymer) added with olive leaf extract as an antimicrobial alternative for topical application in chronic wounds, meeting the great concern of the medical and pharmaceutical industry, regarding the healing of chronic wounds in immunosuppressed patients

2. Material and Methods

2.1. Material

Chitosan (Oakwood Chemical) (Himedia, WF, Pelotas, RS, Brazil) was used with a molar mass of 170.7–198.5 kDa and a degree of deacetylation of 95%. Glycerol (Alphatec, WF, Pelotas, RS, Brazil) was used as a plasticizer to improve membrane flexibility. For the chitosan dilution, 1M acetic acid (Synth) (Alphatec, WF, Pelotas, RS, Brazil) was used. Brain Heart Infusion (BHI) agar (Himedia, WF, Pelotas, RS, Brazil) was used for disk diffusion analysis.

2.2. Olive Leaf Extract (EFO)

Olive leaves (*Olea europaea* L.) of the Arbequina cultivar (Pinheiro Machado—RS, Brazil 31°30'04.0" S, 53°30'42.0" W) were collected and cleaned with 2% sodium hypochlorite and sterile distilled water [21]. The leaves were dried in an oven with forced air circulation at 313.15 K for 24 h, vacuum packed, and stored at room temperature. Before use, they were milled and sieved (diameter less than 0.272 mm). The extract was obtained by the maceration method (1:50 *m/v* of sterile distilled water) for 2 h with gentle agitation at a

temperature of 353.15 K, a condition optimized by Martiny et al. [20]. The extract obtained was vacuum filtered.

2.3. Production of Membranes

The film-forming solutions were prepared by the casting method with 1% (*m/v*) of chitosan, previously dissolved in 25 mL of 1M acetic acid solution for 24 h at 298.15 K and 20% glycerol (based on chitosan mass) [22]. Membranes without the extract were produced as a control adding 25 mL of water distilled and called MQC, while membranes with the extract were obtained with 25 mL of extract and called MQE. The filmogenic solutions were poured into 150 mm diameter acrylic plates and subjected to dehydration in an oven at 313.15 K for 24 h. The membranes were stored at 50% relative humidity for 48 h before the characterization analyses.

2.4. Characterization of Membranes

2.4.1. Thickness

Ten random thickness measurements were taken over a fixed area of the membranes using a digital micrometer (DIGIMESS 0.01 mm), and the results were expressed as the mean \pm standard deviation of these measurements.

2.4.2. Mechanical Properties

The tensile strength (TS) and elongation at break (EB) were obtained according to the standard [23]. Rectangular specimens measuring 25 \times 100 mm of membranes were subjected to stress analysis using a texturometer (TA.XP2i, SMD, GBR) and a 50 N load cell. An initial distance between the clamps of the equipment of 50 mm and a speed of distance between them of 50 mm \cdot min^{−1} were fixed.

2.4.3. Scanning Electron Microscopy

Membrane morphology was observed using a scanning electron microscope (CARL ZEISS—EVO MA10, MA, USA). The samples were analyzed at an accelerating voltage of 20 kV up to a magnification of 2000 \times .

2.4.4. Water Vapor Permeability (WVP)

Permeability was determined gravimetrically by the standard method E96/E96M—14 [24] through capsules containing calcium chloride (CaCl₂). The set was placed in a chamber with a relative humidity of 50%. Calcium chloride mass gain was measured after 10 days. The water vapor permeability of the membranes was quantified using Equation (1):

$$P_{va} = \frac{M_p \cdot L}{t \cdot A \cdot \Delta P} \quad (1)$$

P_{va} is the permeability to water vapor ($\frac{kg}{Pa \cdot s \cdot m}$), M_p is the mass of absorbed moisture (g), L is the film thickness (m), t represents the time of the experiment (seconds), A exposed surface area of the film (m²), and ΔP the partial pressure difference across the film (Pa).

2.4.5. Solubility

Samples of 25 mm diameter membranes were submitted to an oven at 378.15 K for 24 h. Afterward, they were immersed in 50 mL of distilled water and subjected to orbital agitation at 175 rpm for 24 h at a temperature of 298.15 K. A new drying of the samples was performed, and the solubility was expressed from Equation (2) [25].

$$SA = \left(\frac{m_i - m_f}{m_i} \right) \cdot 100 \quad (2)$$

SA (%) of water solubility, m_i is the initial dry mass and m_f is the final dry mass.

2.4.6. Swelling

Membranes measuring 25×25 mm were used as specimens, which were weighed and immersed in distilled water (298.15 K) for 2 min. Wet samples were wiped with paper towels to absorb excess moisture and re-weighed. The amount of water absorbed was calculated using Equation (3) [22].

$$\text{Swelling}(\%) = \frac{100(m_2 - m_1)}{m_1} \quad (3)$$

m_1 and m_2 the masses (g) of the wet and dry samples, respectively.

2.4.7. Fluid Drainage Capacity (FDC)

For FDC, the BS EM 13726-1 method was used for hydrocolloids and dressings [26]. A solution containing $142 \text{ mmol} \cdot \text{L}^{-1}$ of sodium ions and $2.5 \text{ mmol} \cdot \text{L}^{-1}$ of calcium ions was prepared, identified by simulated exudate fluid (FES), which simulates the concentration of sodium and calcium ions frequently found in exudates of wounds. The membranes were conditioned for 48 h at 50% relative humidity prior to the tests. Then, they were cut into 27 mm diameter discs, weighed, placed in a container containing 20 mL of FES, and fixed with a sealing ring. The containers containing the membranes were weighed, inverted so that the samples were in contact with the FES, and kept at 310.15 K for 24 h in a desiccator containing silica gel. At the end of this period, the system was kept at room temperature for 30 min, and the cups were weighed again. The fluid drainage capacity (FDC) was determined using Equation (4):

$$\text{CDF} = \frac{m_{is} - m_{fs}}{t \cdot A} + \frac{m_{im} - m_{fm}}{t \cdot A} \quad (4)$$

m_{is} is the initial mass of the system (g), m_{fs} is the final mass of the system after the drainage period (g), m_{im} the initial mass of the membrane (g), m_{fm} is the final mass of the membrane after the draining period (g), A is the contact area between the membrane and the fluid (m^2), and t is the elapsed time (h).

2.4.8. FTIR-ATR Analysis

For the analysis of infrared spectroscopy with attenuated total reflectance Fourier-transform (FTIR-ATR)(Shimadzu, Prestige 21, Nakagyo-ku, Kyoto, Japão), a Perkin-Elmer spectrometer (UATR Two) was used, ranging from 400 cm^{-1} to 4000 cm^{-1} , with 32 scans per spectrum and resolution of 4 cm^{-1} . This analysis allows the detection of chemical groups present in the analyzed structures.

2.4.9. Anti-Bacterial Property

The adapted disk diffusion method described by NCCLS [27] was used for direct contact. Brain Heart Infusion Agar (BHI) was used as a culture medium, inoculated with the indicator strains *Escherichia coli* (ATCC 11229) and *Staphylococcus aureus* (ATCC 12598) standardized to approximately 10^4 CFU/mL. The contamination occurred by spreading the bacterial culture on the surface (200 μL), and the plates were incubated inverted at 308.15 K. The produced membranes (MQP) and (MWE50%) were cut into 6 mm diameter discs, sterilized in ultraviolet light for 15 min, and added to the Petri plates containing the agar contaminated by the indicative microorganisms (*E. coli* and *S. aureus*). After 24 h of incubation, the zones of inhibition formed were measured using a digital caliper.

2.4.10. Statistical Analysis

All data collected were presented with mean \pm standard deviation and statistically analyzed by the one-way ANOVA test and subsequent t-test with a confidence level of 95%.

3. Results and Discussion

The synthesized membranes were easy to handle without disruption. The standard membrane was transparent, while the membrane incorporated from the olive leaf extract showed a golden-yellow color due to the color of the extract (Figure 1C). Both membranes are uniform and were easily removed from the Petri dish.

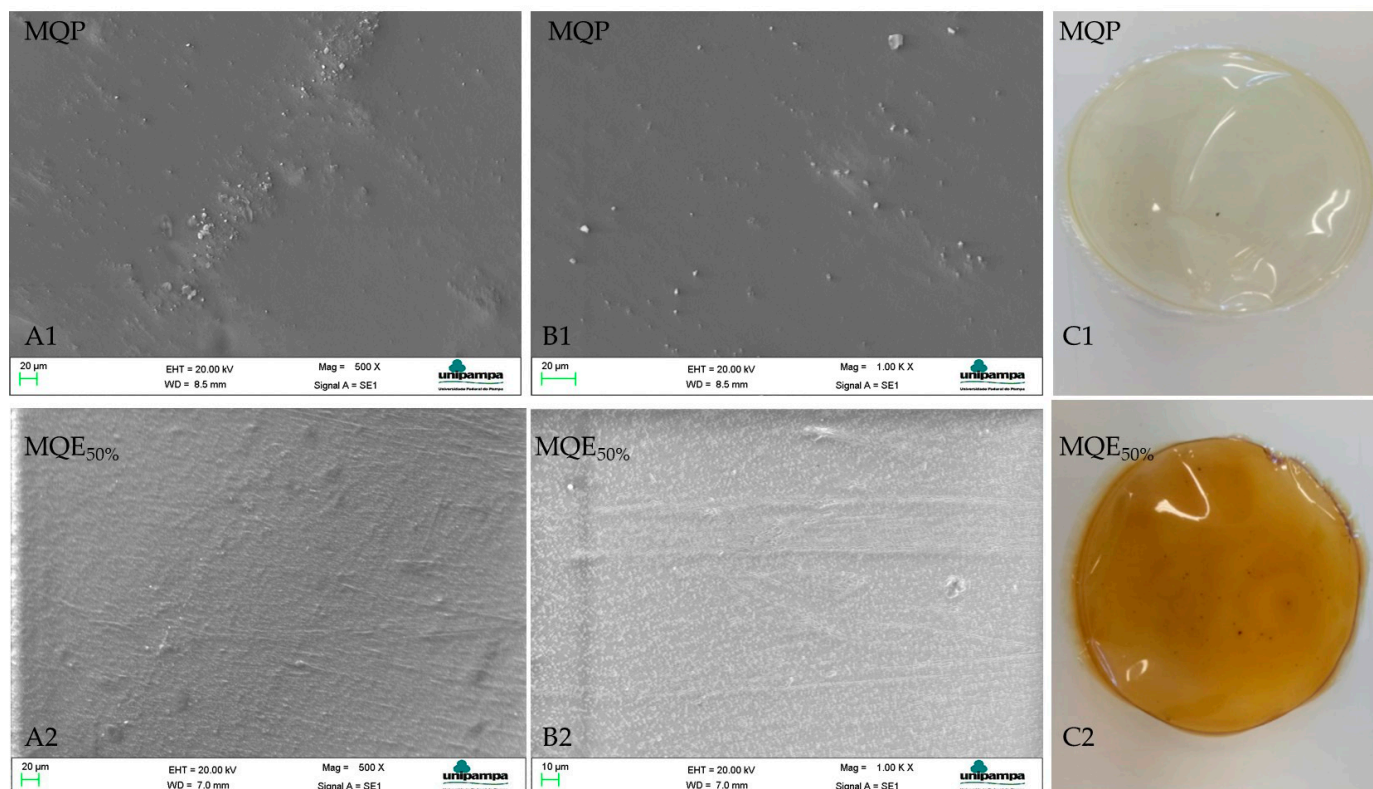


Figure 1. Morphologies for membranes (MQP) and (MQE50%). Letters (A1,A2,B1,B2) represent the SEM images magnifications of 500 \times and 1000 \times , respectively. The letter (C1,C2) represents the membranes developed.

The thickness (Table 1) corresponds to 0.211 ± 0.023 mm for (MQP) and 0.277 ± 0.027 mm for (MQE50%) showing a statistical difference between the membranes. The addition of the extract contributed to a 31.3% increase in thickness due to the compounds present in it, such as oleuropein, hydroxytyrosol, verbascoside, Apigenin-7-glycoside, and Luteolin-7-glycoside, among others [28]. The same behavior was observed by Riaz et al. [29], Contessa et al. [30], and Crizel et al. [31]. Riaz et al. [29] report that the thickness can be increased due to the polymer bonds with the extract compounds with short-distance bonds. Khaliq et al. [32] developed healing membranes based on chitosan and K-carrageenan with thicknesses also in the range from 0.142 to 0.21 mm. Wang et al. [33] developed acetylated glucomannan Konjac membranes for application in dressings, also with a thickness of around 0.2 mm.

The dressing must have sufficient mechanical properties to maintain its integrity during use. The tensile strength of healthy skin ranges from 2.5 to 35 MPa, and elongation ranges from 70% to 78% [32,34]. The rupture tension (Table 1) of the membranes in this study corresponds to 72.41 ± 14.31 and 30.17 ± 8.73 MPa for MQP and MQE50%, representing values with the potential application. The tensile strength decreased significantly with the addition of the extract, which is attributed to the interaction of the extract with the polymer matrix, creating gaps that favor rupture, thus decreasing the tensile strength [35]. The same behavior was observed by Jamroz et al. [36] and Jamroz et al. [37] when adding blueberry extract to chitosan and furcellaran films. The elasticity of the membranes (Table 1),

represented by the elongation at break, however, showed lower values than human skin, corresponding to 41.69 ± 8.14 and $38.64 \pm 3.59\%$ for MQP and MQE50% without statistical difference. Khaliq et al. [32] also found values around 40% for the elasticity of the membranes they developed. Jamróz et al. [37] also reported an elasticity of around 40% in their membranes. Geneviro et al. [38] point out, however, that elongation values around 40% are sufficient to resist natural skin deformations. In this sense, the membranes produced in this study, with regard to mechanical properties, are candidates for application as in vivo healing membranes.

Table 1. Characterization of membranes (MQP) and (MQE_{50%}).

	MQP	MQE _{50%}
TS (Mpa)	72.41 ± 14.31^a	30.17 ± 8.73^b
EB (%)	41.69 ± 8.14^a	38.64 ± 3.59^a
Thickness (mm)	0.211 ± 0.023^b	0.277 ± 0.027^a
WVP ($\text{kg} \cdot \text{m}^{-1} \cdot \text{Pa}^{-1} \cdot \text{s}^{-1}$)	0.39 ± 0.1^a	0.52 ± 0.22^a
Solubility (%)	18.56 ± 1.64^b	34.71 ± 2.62^a
Swelling (%)	249.49 ± 4.77^a	57.42 ± 1.13^b
FDC ($\text{g} \cdot \text{m}^{-2} \cdot \text{h}^{-1}$)	22.75 ± 4.80^b	29.31 ± 1.65^a

^{a, b} Different letters on the same line indicate a statistically significant difference ($p \leq 0.05$) between the means by the *t*-test.

The morphological analysis (Figure 1) showed a smooth and homogeneous surface for the synthesized membranes. MQP showed some point clusters in the matrix. Zhang et al. [39] report that chitosan films dissolved in non-hydroxylated acids such as acetic acid tend to exhibit this behavior, explained by intermolecular interactions between chitosan and non-hydroxylated acid anions. The addition of the extract minimized the presence of agglomerates, possibly by supplying hydroxyls from the aqueous extract. In chitosan films used from hydroxylated acids, the structures are homogeneous and smooth, as there is a greater release of protons that favor strong interactions with the protonated chitosan chains [40].

A good dressing must be efficient in absorbing exudates; however, it is important that they prevent water loss from the wound, providing a moist environment and thus aiding healing [41]. The water vapor permeability (Table 1) showed no significant difference between the membranes. The values found in this study are below those found by Razzaq et al. [42] in barley β -glucan and ZnO membranes for wound healing, explained by their more compact structure, which increases the diffusion path of the molecules and consequently a lower permeability. However, low permeability to water vapor in healing membranes prevents the wound from becoming too wet due to possible external humidity; in this sense, the membrane acts as an obstacle to water vapors coming from the external environment.

The solubility of MQE_{50%} increased in relation to MQP, which is explained by the hydrophilicity of the extract since it is an aqueous extract. The same behavior was reported by Narasagoudr et al. [43] on chitosan and poly (vinyl alcohol) films and Contessa et al. [22] on chitosan and agar-agar blends. Pacheco et al. [44], in multilayer membranes of fibroin + chitosan + alginate to release diclofenac sodium, obtained a solubility of around 73% in a period of seven days of analysis, resulting in the complete dissolution of one of the layers. Therefore, the solubility of the MQE_{50%} membrane, although increased, still remains suitable for cutaneous application since it remained intact after the analysis (24 h), with the weight loss coming from the solubility of the plasticizer used. According to Ma et al. [45], this behavior is expected because glycerol is completely miscible in water.

Swelling is the ability of the film to retain liquid; in the healing process, there is the production of wound exudates [46]. Excess exudates compromise cell proliferation, so it is important that the dressing is efficient in absorbing these exudates [47]. The values obtained indicate that there was a significant decrease in the swelling of the MQE_{50%} in

relation to the MQP. Similar behavior to that found by Riaz et al. [29] in chitosan-based films with Chinese chive root extract, where they also observed a reduction in the degree of swelling with the addition of the extract, from 57.38% to 40.49%, was explained by the presence of hydroxyl groups (hydrophilic groups) in the chitosan molecule. Yu et al. [48], in curative membranes, obtained values of around 39 and 58% in 24 h of analysis for chitosan–collagen/montmorillonite and chitosan–collagen/organomontmorillonite membranes, respectively, and considered the swelling properties to be good. This study evaluated swelling in just 2 min, and the results were similar for MQE_{50%} and much higher for MQP, indicating that both have the potential for application as skin dressings.

The FDC represents the amount of fluid released from the wound that the dressing can drain, either by absorption or vapor permeation. Dressings with very high FDC can lead to wound dehydration, while very low values can generate an accumulation of exudates, causing healing problems [44]. Commercial dressings range from 12,350 to 1670 g/m² 24h; third-degree burns generally generate from 3400 to 5100 g of exudates per day [49]. Thus, the values found for MQP and MQE_{50%} membranes (22.75 ± 4.80 and 29.31 ± 1.65 g·m⁻²·h⁻¹) can be used in wounds with mild and moderate exudate production.

The FDC, as already explained, is the ability to drain exudates from the wound; the way our membrane does this drainage is mostly through its swelling and not by transferring it to water vapor due to low permeability (0.52 ± 0.22 kg·m⁻¹·Pa⁻¹·s⁻¹) evidenced in this study. This is a promising result since the membranes, over time, absorb the released exudates and do not transfer liquids to the outside of the wound, getting aesthetically more presentable.

The analysis of membrane functional groups was investigated by FTIR-ATR analysis (Figure 2). The spectra of the MQP and MQE_{50%} membranes showed absorption peaks at extremely similar wave numbers, indicating a slight increase in MQE_{50%} around 3500 cm⁻¹. The peak around 3423 cm⁻¹ is very characteristic of stretching vibrations of the OH group [50]. When superimposed, the spectrum of the MQE_{50%} membrane showed an increase in peak intensity in the same absorption band, indicating the formation of bonding of the OH groups of oleuropein, which has an abundance of this group, with the other constituents of the membrane (chitosan + glycerol). The same was observed by Azar et al. [51] in sodium pectin–caseinate hydrogel containing olive leaf extract as a nano lipid carrier. Peaks 2946–2874 cm⁻¹ correspond to CH stretching vibrations [52]. Absorption around 1635 cm⁻¹ is related to the stretching of carbonyl groups (C=O) [53] and characteristic of the –N=C– bond in chitosan hydrogels [54]. The peak around 1552 cm⁻¹ was also found by Fang et al. [55] in chitosan hydrogel and is characteristic of the –C=C– bond. Peaks around 1552 cm⁻¹ are indicative of the presence of the amine (–NH) characteristic of chitosan [22]. Peaks around 1044 cm⁻¹ correspond to the glycosidic bonds of chitosan [52].

The anti-bacterial analysis did not indicate a zone of inhibition of the control membrane without the active extract (Figure 3) for the microbiota tested. Some studies report the same behavior. Sugumar et al. [55] and Contessa et al. [22] explain that chitosan has an anti-bacterial effect when the target organism is in direct contact with its active sites. The contact of the amino group with the cell wall of the microorganism is necessary. The structure of the membrane makes this direct contact impossible because chitosan cannot diffuse [56].

The zone of inhibition is characterized by the absence of bacterial growth around the membranes. The MQP_{50%} showed a zone of inhibition for the two microorganisms tested without significant differences. This is a very promising result since not all extracts are efficient on gram-positive and gram-negative walls; due to differences in cell wall structure [57], they are generally effective against a group of cell walls [48]. In general, chronic infections, inflammation, or prolonged healing are due to the contamination of wounds by *E. coli* and *S. aureus*. Dressings with an anti-bacterial effect against these strains have great potential for application [58]. Mayer et al. [59], when analyzing the anti-bacterial activity of curative membranes of 2,3-dialdehyde cellulose with gelatin and zein, obtained inhibition halos of 5.2 ± 0.1 mm for *E. coli* and 4.6 ± 0.2 for *S. aureus*. Rao et al. [58] also

obtained inhibition halos around 8.15% for *S. aureus* and 14.55% for *E. coli* in curative membranes based on carboxymethyl chitosan and polyvinyl alcohol.

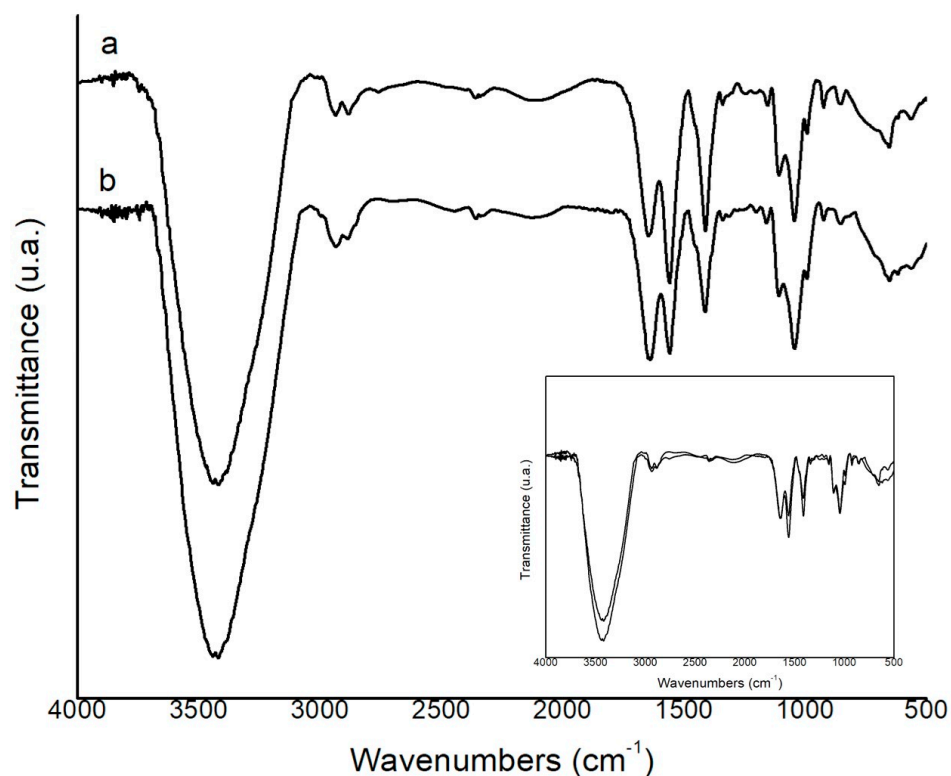


Figure 2. Fourier–transform infrared (FTIR) spectra of (a) MPQ and (b) MQE_{50%}.

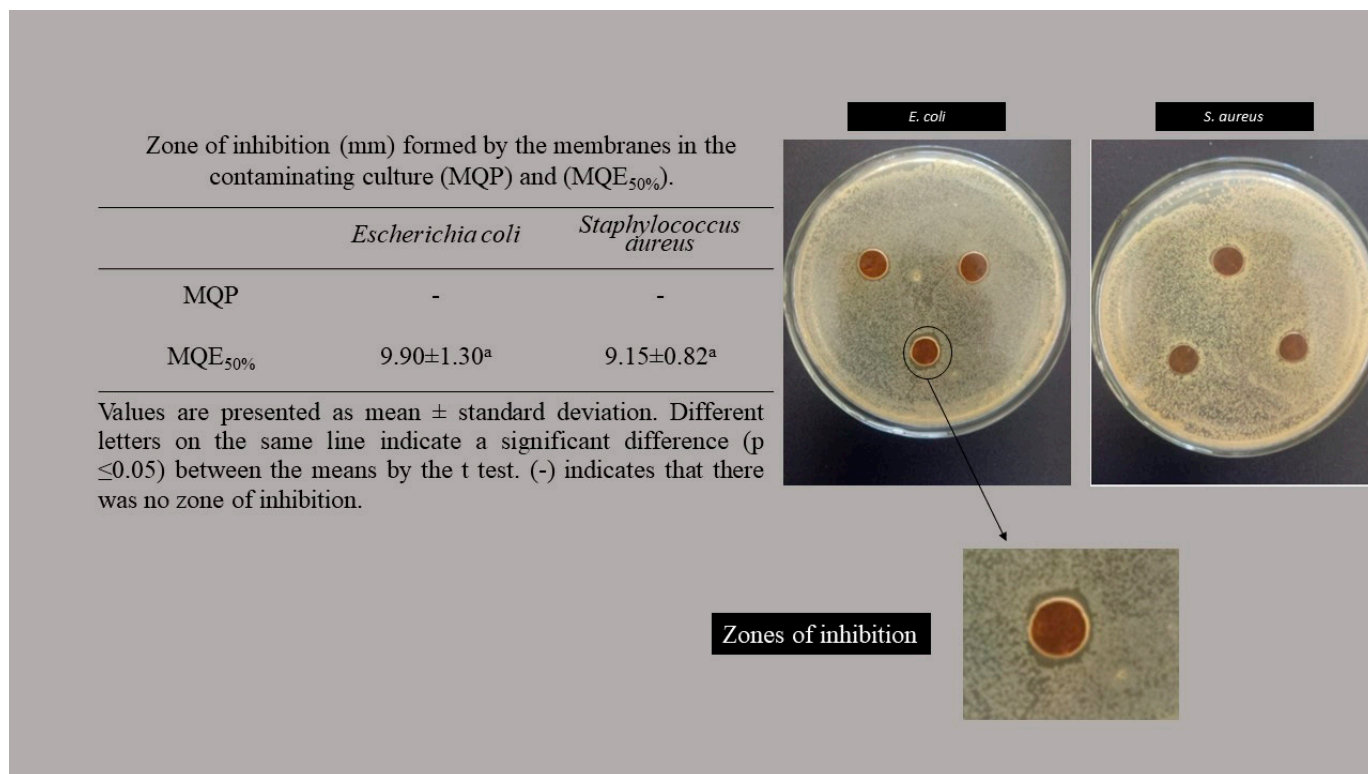


Figure 3. Zone of inhibition (mm) formed by the membranes in the contaminating culture (MQP) and (MQE_{50%}).

In view of the above, we can report that the chitosan-based membrane, added with olive leaf extract developed in this study, presented adequate handling characteristics, fluid drainage capacity, and antimicrobial activity against two of the most worrisome bacteria when it comes to skin infections. Therefore, this work reports an antimicrobial membrane with great potential for application in chronic wounds.

4. Conclusions

In this work, a chitosan-based membrane added with olive leaf extract was developed for potential application as an antimicrobial membrane for wound application. The addition of the extract to the membrane provided a reduction in the tensile strength and swelling, however the values still present ideal characteristics for the application (30.17 ± 8.73 MPa e $38.64 \pm 3.59\%$ for tensile strength and elongation, respectively). The addition of the extract contributed to the increase in fluid drainage capacity, promoting an improvement in wound healing (29.31 ± 1.65 g·m⁻²·h⁻¹). In addition, the membrane added with extract showed anti-bacterial properties for strains of *E. coli* and *S. aureus*. All the results indicated that the developed membrane showed viable characteristics for use as a wound dressing since it has adequate mechanical properties, absorption of exudates, and anti-bacterial activity against the most common bacteria in skin wounds.

Author Contributions: R.C.A.: Conceptualization, methodology. C.R.C.: Conceptualization, writing, original draft preparation, proofreading, and editing. C.C.M.: Project management, supervision, writing, and editing. G.S.d.R.: Project Management, supervision, formal review, and review. All authors have read and agreed to the published version of the manuscript.

Funding: The authors are grateful for FAPERGS (Foundation Research Support in the State of Rio Grande do Sul), CNPq (National Council of Science and Technological Development), and the support of the Coordination of Improvement of Higher-Level Personnel—Brazil (CAPES) (Financing Code 001).

Institutional Review Board Statement: Not applicable.

Informed Consent Statement: Not applicable.

Data Availability Statement: All data generated or analyzed during this study are included in this published article.

Conflicts of Interest: The authors confirm that this is an original research article and that no conflict of interest is associated with this publication. All authors have read and approved the MS and are aware of its submission to JFST.

References

1. Williams, P.L.; Bannister, L.H.; Berry, M.M.; Collins, P.; Dyson, M.; Dussek, J.E. *Gray's Anatomy—International Student Edition*, 38th ed.; Churchill Livingstone: Oxford, UK, 1995.
2. Agwa, M.M.; Sabra, S.; Atwa, N.A.; Dahdooh, H.Á.; Lithy, R.M.; Elmotasem, H. Potential of frankincense essential oil-loaded whey protein nanoparticles embedded in frankincense resin as a wound healing film based on green technology. *J. Drug Deliv. Sci. Technol.* **2022**, *71*, 103291. [\[CrossRef\]](#)
3. Oliveira, J.G.F.; Lira, M.M.; Souza, T.L.; Campos, S.B.; Lemes, A.C.; Egea, M.B. Plant-based mucilage with healing and anti-inflammatory actions for topical application: A review. *Food Hydrocoll. Health* **2021**, *1*, 100012. [\[CrossRef\]](#)
4. Liang, Y.; Liang, Y.; Zhang, H.; Guo, B. Antibacterial biomaterials for skin wound dressing. *Asian J. Pharm. Sci.* **2022**, *24*, 353–384. [\[CrossRef\]](#) [\[PubMed\]](#)
5. Ousey, K. The role of topical metronidazole in the management of infected wounds. *Wounds* **2018**, *14*, 105–109.
6. Abdel-Sayed, P.; Hirt-Burri, N.; Roessingh, A.B.; Raffoul, W.; Applegate, L.A. Evolution of Biological Bandages as First Cover for Burn Patients. *Adv. Wound Care* **2019**, *8*, 555–564. [\[CrossRef\]](#) [\[PubMed\]](#)
7. Savencu, I.; Iurian, S.; Porfire, A.; Bogdan, C.; Tomuta, I. Review of advances in polymeric wound dressing films. *React. Funct. Polym.* **2021**, *168*, 105059. [\[CrossRef\]](#)
8. Varaprasad, K.; Jayaramudu, T.; Kanikireddy, V.; Toro, C.; Sadiku, E.R. Alginate-based composite materials for wound dressing application: A mini review. *Carbohydr. Polym.* **2020**, *236*, 116025. [\[CrossRef\]](#)
9. Moholkar, D.N.; Sadalage, P.S.; Peixoto, D.; Paiva-Santos, A.C.; Pawar, K.D. Recent advances in biopolymer-based formulations for wound healing applications. *Eur. Polym. J.* **2021**, *160*, 110784. [\[CrossRef\]](#)

10. Jayakumar, R.; Prabakaran, M.; Kumar, P.T.S.; Nair, S.V.; Tamura, H. Biomaterials based on chitin and chitosan in wound dressing applications. *Biotechnol. Adv.* **2011**, *29*, 322–337. [CrossRef]
11. Khan, Z.A.; Jamil, S.; Akhtar, A.; Mustehsan, B.; Yar, M. Chitosan based hybrid materials used for wound healing applications- A short review. *Int. J. Polym. Mater. Polym. Biomater.* **2020**, *69*, 419–436. [CrossRef]
12. Oliveira, A.L.S.; Gondim, S.; Gómez-García, R.; Ribeiro, T.; Pintado, M. Olive leaf phenolic extract from two Portuguese cultivars –bioactivities for potential food and cosmetic application. *J. Environ. Chem. Eng.* **2021**, *9*, 106175. [CrossRef]
13. Rosa, G.S.; Martiny, T.R.; Dotto, G.L.; Vanga, S.K.; Parrine, D.; Gariepy, Y.; Lefsrud, M.; Raghavan, V. Eco-friendly extraction for the recovery of bioactive compounds from Brazilian olive leaves. *Sustain. Mater. Technol.* **2021**, *28*, e00276. [CrossRef]
14. Difonzo, G.; Pasqualone, A.; Silletti, R.; Cosmai, L.; Summo, C.; Paradiso, V.M.; Caponio, F. Use of olive leaf extract to reduce lipid oxidation of baked snacks. *Food Res. Int.* **2018**, *108*, 48–56. [CrossRef]
15. Jimenez-lopez, C.; Carpena, M.; Lourenço-Lopes, C.; Gallardo-Gomez, M.; Lorenzo, J.M.; Barba, F.J.; Prieto, M.A.; Simal-Gandara, J. Bioactive Compounds and Quality of Extra Virgin Olive Oil. *Foods* **2020**, *9*, 1014. [CrossRef]
16. Rocchetti, G.; Callegari, M.L.; Senizza, A.; Giuberti, G.; Ruzzolini, J.; Romani, A.; Urciuoli, S.; Nediani, C.; Lucini, L. Oleuropein from olive leaf extracts and extra-virgin olive oil provides distinctive phenolic profiles and modulation of microbiota in the large intestine. *Food Chem.* **2022**, *380*, 132187. [CrossRef] [PubMed]
17. Papoti, V.T.; Papageorgiou, M.; Dervisi, K.; Alexopoulos, E.; Apostolidis, K.; Petridis, D. Screening Olive Leaves from Unexploited Traditional Greek Cultivars for Their Phenolic Antioxidant Dynamic. *Foods* **2018**, *7*, 197. [CrossRef]
18. Abi-Khattar, A.M.; Boussetta, N.; Rajha, H.N.; Abdel-Massih, R.M.; Louka, N.; Maroun, R.G.; Vorobiev, E.; Debs, E. Mechanical damage and thermal effect induced by ultrasonic treatment in olive leaf tissue. Impact on polyphenols recovery. *Ultrason. Sonochem.* **2022**, *82*, 105805. [CrossRef]
19. Romani, A.; Ieri, F.; Urciuoli, S.; Noce, A.; Marrone, G.; Nediani, C.; Bernini, R. Health Effects of Phenolic Compounds Found in Extra-Virgin Olive Oil, By-Products, and Leaf of *Olea europaea* L. *Nutrients* **2019**, *11*, 1776. [CrossRef]
20. Martiny, T.R.; Raghavan, V.; Moraes, C.C.; Rosa, G.S.; Dotto, G.L. Optimization of green extraction for the recovery of bioactive compounds from Brazilian olive crops and evaluation of its potential as a natural preservative. *J. Environ. Chem. Eng.* **2021**, *9*, 105130. [CrossRef]
21. Rosa, G.S.; Vanga, S.K.; Gariepy, Y.; Raghavan, V. Development of biodegradable films with improved antioxidant properties based on the addition of carrageenan containing olive leaf extract for food packaging applications. *J. Polym. Environ.* **2019**, *28*, 123–130. [CrossRef]
22. Contessa, C.R.; Rosa, G.S.; Moraes, C.C. New Active Packaging Based on Biopolymeric Mixture Added with Bacteriocin as Active Compound. *Int. J. Mol. Sci.* **2021**, *22*, 10628. [CrossRef]
23. ASTM D882-18; Standard Test Method for Tensile Properties of Thin Plastic Sheeting. Annual Book of ASTM Standards. ASTM: Philadelphia, PA, USA, 2018.
24. ASTM E96/E96M-16; Standard Test Methods for Water Vapor Transmission of Materials. Annual Book of ASTM Standards. ASTM: Philadelphia, PA, USA, 2016.
25. Riaz, A.; Lei, S.; Akhtar, H.M.S.; Wan, P.; Chen, D.; Jabbar, S.; Abid, M.; Hashim, M.M.; Zeng, X. Preparation and characterization of chitosan-based antimicrobial active food packaging film incorporated with apple peel polyphenols. *Int. J. Biol. Macromol.* **2018**, *114*, 547–555. [CrossRef]
26. BS EN 13726-1:2002; Test Methods for Primary Wound Dressings. Part 1: Aspects of Absorbency, Fluid Handling Capacity. British Standards Institute—BSI: London, UK, 2002.
27. NCCLS. Performance Standards for Antimicrobial Disk Susceptibility Tests; Approved Standard. NCCLS Document M2-A8. Pennsylvania, USA. 2003. Available online: http://www.anvisa.gov.br/servicosau/manuel/csl/csl_OPASM2-A8.pdf (accessed on 22 March 2023).
28. Benavente-Garcia, O.; Castilho, J.; Lorente, J.; Ortuno, A.; Rio, J.A. Antioxidant activity of phenolics extracted from *Olea europaea* L. leaves. *Food Chem.* **2000**, *68*, 457–462. [CrossRef]
29. Riaz, A.; Lagnika, C.; Luo, H.; Dai, Z.; Nie, M.; Hashim, M.M.; Liu, C.; Song, J.; Li, D. Chitosan-based biodegradable active food packaging film containing Chinese chive (*Allium tuberosum*) root extract for food application. *Int. J. Biol. Macromol.* **2020**, *150*, 595–604. [CrossRef]
30. Contessa, C.R.; Souza, N.B.; Gonçalves, G.B.; Moura, C.M.; Rosa, G.S.; Moraes, C.C. Development of Active Packaging Based on Agar-Agar Incorporated with Bacteriocin of *Lactobacillus sakei*. *Biomolecules* **2021**, *11*, 1869. [CrossRef]
31. Crizel, T.M.; Rios, A.O.; Alves, V.D.; Bandarra, N.; Moldão-Martins, M.; Flores, S.H. Active food packaging prepared with chitosan and olive pomace. *Food Hydrocoll.* **2018**, *74*, 139–150. [CrossRef]
32. Khaliq, T.; Sohail, M.; Minhas, M.U.; Shah, A.S.; Jabeen, N.; Khan, S.; Hussain, Z.; Mahmood, A.; Kousar, M.; Rashid, H. Self-crosslinked chitosan/ κ -carrageenan-based biomimetic membranes to combat diabetic burn wound infections. *Int. J. Biol. Macromol.* **2022**, *197*, 157–168. [CrossRef] [PubMed]
33. Wang, C.; Li, B.; Chen, T.; Mei, N.; Wang, X.; Tanq, S. Preparation and bioactivity of acetylated konjac glucomannan fibrous membrane and its application for wound dressing. *Carbohydr. Polym.* **2020**, *229*, 115404. [CrossRef] [PubMed]

34. Annaidh, A.N.; Bruyere, K.; Destrade, M.; Gilchrist, M.; Otténio, M. Characterization of the anisotropic mechanical properties of excised human skin. *J. Mech. Behav. Biomed. Mater.* **2012**, *5*, 139–148. [\[CrossRef\]](#)
35. Hassan, A.; Niazi, M.B.K.; Hussain, A.; Farrukh, S.; Ahmad, T. Development of Anti-bacterial PVA/Starch Based Hydrogel Membrane for Wound Dressing. *J. Polym. Environ.* **2018**, *26*, 235–243. [\[CrossRef\]](#)
36. Jamróz, E.; Janik, M.; Juszcak, L.; Kruk, T.; Kulawik, P.; Szuwarzynski, M.; Kawecka, A.; Khachatryan, K. Composite biopolymer films based on a polyelectrolyte complex of furcellaran and chitosan. *Carbohydr. Polym.* **2021**, *274*, 118627. [\[CrossRef\]](#) [\[PubMed\]](#)
37. Jamróz, E.; Tkaczewska, J.; Juszcak, L.; Zimoswska, M.; Kawecka, A.; Krzysciak, P.; Skora, M. The influence of lingonberry extract on the properties of novel, double-layered biopolymer films based on furcellaran, CMC and a gelatin hydrolysate. *Food Hydrocoll.* **2022**, *124*, 107334. [\[CrossRef\]](#)
38. Genevro, G.M.; Gomes, N.R.J.; Paulo, L.A.; Lopes, P.S.; Moraes, M.A.; Beppu, M.M. Glucomannan asymmetric membranes for wound dressing. *J. Mater. Res.* **2019**, *34*, 481–489. [\[CrossRef\]](#)
39. Zhang, T.; Xu, H.; Zhang, Y.; Zhang, Z.; Yang, X.; Wei, Y.; Huang, D.; Lian, X. Fabrication and characterization of double-layer asymmetric dressing through electrostatic spinning and 3D printing for skin wound repair. *Mater. Des.* **2022**, *128*, 110711. [\[CrossRef\]](#)
40. Soares, L.S.; Perim, R.B.; Alvarenga, E.S.; Guimarães, L.M.; Teixeira, A.V.N.C.; Coimbra, J.S.R.; Oliveira, E.B. Insights on physicochemical aspects of chitosan dispersion in aqueous solutions of acetic, glycolic, propionic or lactic acid. *Int. J. Biol. Macromol.* **2019**, *128*, 140–148. [\[CrossRef\]](#)
41. Alavi, T.; Rezvanian, M.; Ahmad, N.; Mohamad, N.; Shioh-Fern, N. Pluronic-F127 composite film loaded with erythromycin for wound application: Formulation, physicomechanical and in vitro evaluations. *Drug Deliv. Transl. Res.* **2019**, *9*, 508–519. [\[CrossRef\]](#) [\[PubMed\]](#)
42. Razzaq, H.A.A.; Ayala, G.G.; Santagata, G.; Bosco, F.; Mollea, C.; Larsen, N.; Duraccio, D. Bioactive films based on barley β -glucans and ZnO for wound healing applications. *Carbohydr. Polym.* **2021**, *272*, 118442. [\[CrossRef\]](#)
43. Narasagoudr, S.S.; Hegde, V.G.; Chougale, R.B.; Masti, S.P.; Dixit, S. Influence of boswellic acid on multifunctional properties of chitosan/poly (vinyl alcohol) films for active food packaging. *Int. J. Biol. Macromol.* **2020**, *154*, 48–61. [\[CrossRef\]](#)
44. Pacheco, M.S.; Kano, G.E.; Paulo, L.A.; Lopes, P.S.; Moraes, M.A. Silk fibroin/chitosan/alginate multilayer membranes as a system for controlled drug release in wound healing. *Int. J. Biol. Macromol.* **2020**, *152*, 803–811. [\[CrossRef\]](#)
45. Ma, Y.; Xin, L.; Tan, H.; Fan, M.; Li, J.; Jia, Y.; Ling, Z.; Chen, Y.; Hu, X. Chitosan membrane dressings toughened by glycerol to load antibacterial drugs for wound healing. *Mater. Sci. Eng. C* **2017**, *81*, 522–531. [\[CrossRef\]](#)
46. Zhang, W.; Jiang, Q.; Shen, J.; Gao, P.; Yu, D.; Xu, Y.; Xia, W. The role of organic acid structures in changes of physicochemical and antioxidant properties of crosslinked chitosan films. *Food Packag. Shelf Life* **2022**, *31*, 100797. [\[CrossRef\]](#)
47. Khalatbari, E.; Tajabadi, M.; Khavandi, A. Multifunctional exosome-loaded silk fibroin/alginate structure for potential wound dressing application. *Mater. Commun.* **2022**, *31*, 103549. [\[CrossRef\]](#)
48. Yu, X.; Guo, L.; Cao, X.; Shang, S.; Liu, Z.; Huang, D.; Cao, Y.; Cui, F.; Tian, L. *Callicarpa nudiflora* loaded on chitosan-collagen/organomontmorillonite composite membrane for antibacterial activity of wound dressing. *Int. J. Biol. Macromol.* **2018**, *120*, 2279–2284. [\[CrossRef\]](#) [\[PubMed\]](#)
49. Morgado, P.I.; Aguiar-Ricardo, A.; Correia, I.J. Asymmetric membranes as ideal wound dressings: An overview on production methods, structure, properties and performance relationship. *J. Membr. Sci.* **2015**, *490*, 139–151. [\[CrossRef\]](#)
50. Psocchia, E.; Papadopoulos, L.; Gkiliopoulos, D.J.; Francone, A.; Grigora, M.-E.; Tzetzis, D.; de Castro, J.V.; Neves, N.M.; Triantafyllidis, K.S.; Torres, C.M.S.; et al. Bottom-Up Development of Nanoimprinted PLLA Composite Films with Enhanced Antibacterial Properties for Smart Packaging Applications. *Macromol* **2021**, *1*, 49–63. [\[CrossRef\]](#)
51. Azar, F.A.N.; Peseshki, A.; Ghanbarzadeh, B.; Hamishehkar, H.; Mohammadi, M.; Hamdipour, S.; Daliri, H. Pectin-sodium caseinat hydrogel containing olive leaf extract-nano lipid carrier: Preparation, characterization and rheological properties. *LWT* **2021**, *148*, 111757. [\[CrossRef\]](#)
52. Avila, L.B.; Barreto, E.R.C.; Moraes, C.C.; Morais, M.M.; Rosa, G.S. Promising New Material for Food Packaging: An Active and Intelligent Carrageenan Film with Natural Jaboticaba Additive. *Foods* **2022**, *6*, 792. [\[CrossRef\]](#)
53. Panda, P.K.; Yang, J.-M.; Chang, Y.-H.; Su, W.-W. Modification of different molecular weights of chitosan by p-Coumaric acid: Preparation, characterization and effect of molecular weight on its water solubility and antioxidant property. *Int. J. Biol. Macromol.* **2019**, *136*, 661–667. [\[CrossRef\]](#)
54. Fang, W.; Yang, L.; Hong, L.; Hu, Q. A chitosan hydrogel sealant with self-contractile characteristic: From rapid and long-term hemorrhage control to wound closure and repair. *Carbohydr. Polym.* **2021**, *271*, 118428. [\[CrossRef\]](#)
55. Sugumar, S.; Mukhejee, A.; Chandrasekaran, N. Eucalyptus oil nanoemulsion-impregnated chitosan film: Antibacterial effects against a clinical pathogen, *Staphylococcus aureus*, in vitro. *Int. J. Nanomed.* **2015**, *10*, 67–75. [\[CrossRef\]](#)
56. Hafsa, J.; Smach, M.; Khedher, M.R.B.; Charfeddine, B.; Limem, K.; Majdoub, H.; Rouatbi, S. Physical, antioxidant and antimicrobial properties of chitosan films containing *Eucalyptus globulus* essential oil. *LWT Food Sci. Technol.* **2016**, *68*, 356–364. [\[CrossRef\]](#)
57. Panda, P.K.; Sadegui, K.; Kitaee, P.; Seo, J. Regeneration Approach to Enhance the Antimicrobial and Antioxidant Activities of Chitosan for Biomedical Applications. *Polymers* **2023**, *15*, 132. [\[CrossRef\]](#) [\[PubMed\]](#)

58. Rao, K.M.; Sudhakar, K.; Suneetha, M.; Won, S.Y.; Han, S.S. Fungal-derived carboxymethyl chitosan blended with polyvinyl alcohol as membranes for wound dressings. *Int. J. Biol. Macromol.* **2021**, *190*, 792–800. [[CrossRef](#)] [[PubMed](#)]
59. Mayer, S.; Tallawi, M.; Luca, I.; Calarco, A.; Reinhardt, N.; Gray, L.A.; Drechsler, K.; Moeini, A.; Germann, N. Antimicrobial and physicochemical characterization of 2,3-dialdehyde cellulose-based wound dressings systems. *Carbohydr. Polym.* **2021**, *272*, 118506. [[CrossRef](#)]

Disclaimer/Publisher’s Note: The statements, opinions and data contained in all publications are solely those of the individual author(s) and contributor(s) and not of MDPI and/or the editor(s). MDPI and/or the editor(s) disclaim responsibility for any injury to people or property resulting from any ideas, methods, instructions or products referred to in the content.